

# On Quasi-Localized Dual Pairs in Reproducing Kernel Hilbert Spaces

Helmut Harbrecht<sup>1</sup>, Rüdiger Kempf<sup>2</sup>, and Michael Multerer<sup>3</sup>

<sup>1</sup> *Departement Mathematik und Informatik, Universität Basel, Spiegelgasse 1, 4051 Basel, Switzerland*

<sup>2</sup> *Applied and Numerical Analysis, Department of Mathematics, University of Bayreuth, 95440 Bayreuth, Germany*

<sup>3</sup> *Istituto Eulero, Università della Svizzera italiana, Via la Santa 1, 6962 Lugano, Switzerland*

August 22, 2024

## Abstract

In scattered data approximation, the span of a finite number of translates of a chosen radial basis function is used as approximation space and the basis of translates is used for representing the approximate. However, this natural choice is by no means mandatory and different choices, like, for example, the Lagrange basis, are possible and might offer additional features. In this article, we discuss different alternatives together with their canonical duals. We study a localized version of the Lagrange basis, localized orthogonal bases, such as the Newton basis, and multiresolution versions thereof, constructed by means of samplers. We argue that the choice of orthogonal bases is particularly useful as they lead to symmetric preconditioners. All bases under consideration are compared numerically to illustrate their feasibility for scattered data approximation. We provide benchmark experiments in two spatial dimensions and consider the reconstruction of an implicit surface as a relevant application from computer graphics.

## 1 Introduction

Kernel methods have become more and more popular over the years. Applications range from scattered data approximation to machine learning, see for example [11, 43, 46] and the references therein. In general, these methods aim at the reconstruction of an unknown function by only using scattered data, i.e., tuples of data sites and corresponding measurements of the function. Assuming that the data generating process  $f$  is contained in a reproducing kernel Hilbert space  $\mathcal{H}$ , we can always find a set of *dual pairs*  $\{(\phi_i, \tilde{\phi}_i)\}$  such that the orthogonal projection  $s_f$  of  $f$  in  $\text{span}\{\phi_i\}$  can be written as

$$s_f = \sum_{i=1}^N \langle f, \tilde{\phi}_i \rangle_{\mathcal{H}} \phi_i \quad \text{or, equivalently,} \quad s_f = \sum_{i=1}^N \langle f, \phi_i \rangle_{\mathcal{H}} \tilde{\phi}_i.$$

Given a set of data sites  $\{\mathbf{x}_1, \dots, \mathbf{x}_N\}$ , the most commonly known dual pair is  $\{(K(\cdot, \mathbf{x}_i), \chi_i)\}$ . Herein,  $\{K(\cdot, \mathbf{x}_i)\}$ , is the basis of kernel translates induced by the reproducing kernel  $K$  of  $\mathcal{H}$  and  $\chi_i$  is the corresponding Lagrange basis. This specific pair allows the easy representation of the orthogonal projection by the interpolant

$$s_f = \sum_{i=1}^N f(\mathbf{x}_i) \chi_i.$$

This representation has the advantage that it separates the data from the data sites. However, even if we do not consider the cost to compute the Lagrange basis  $\{\chi_i\}$ , every evaluation of the interpolant  $s_f$  entails a cost of  $\mathcal{O}(N^2)$ , since every basis element  $\chi_i$  is a linear combination of

the  $N$  kernel translates that need to be evaluated. Numerically, this is not feasible. Therefore, a framework was established in a series of articles [20, 12, 19] in order to compute localized approximate Lagrange functions for very specific classes of kernels.

In the present article, we give an interpretation of the localization of the Lagrange basis by considering it as an approximation/sparsification of the inverse of the kernel matrix  $\mathbf{A} = [K(\mathbf{x}_i, \mathbf{x}_j)]$  by means of a very specific pattern, which we call *footprint*. This approximate inverse is typically not symmetric although the kernel matrix itself is. Hence, we cannot use it as a preconditioner in a conjugate gradient method. To address this issue, we discuss modifications of the approach by involving the matrix square root of the footprints or their Cholesky decomposition. In the limit, for growing footprint size, both approaches yield orthonormal basis functions, which means that  $\tilde{\phi}_i = \phi_i$  for  $i = 1, \dots, N$ . Particularly, the second approach is a localized version of the Newton basis, see [35]. Either choice may then be used to construct symmetric and sparse preconditioners for notoriously bad conditioned kernel matrices, e.g., issuing from the widely used Matérn kernels.

A multiresolution approach for the construction of dual pairs, that we consider here, are samplelets [21]. Samplelets are discrete signed measures constructed such that polynomials up to a degree of our choice vanish. Therefore, the kernel matrix becomes quasi-sparse in samplelet coordinates and can be compressed to a sparse matrix. The resulting matrix pattern is finger band structured with easy to compute Cholesky decomposition whence a graph based reordering strategy is used [21]. Furthermore, it has been shown in [23] that samplelets establish even a sparse arithmetic for kernel matrices, enabling efficient scattered data analysis.

This article is organized as follows. In Section 2, we recall the basics of scattered data approximation and the setting we are studying. In Section 3, we recall general dual pairs and the Lagrange basis in particular. Moreover, we discuss their connection to the theory of pseudo-differential operators. This gives an alternative point of view to important properties of kernel matrices which we want to use in the subsequent section. There, in Section 4, we consider alternative dual pairs. First, in Section 4.1, we give a review of the quasi-localization of the Lagrange basis by using the exponential decay of the inverse kernel matrix. Then, we use these ideas to derive a new way to construct preconditioners for kernel matrices in Section 4.2. The underlying basis functions are orthonormal, including especially a localized version of the Newton basis. As an alternative approach, we review the basics of samplelets in Section 5. In Section 6, we compare the different dual pairs under consideration numerically. Extensive numerical tests in two and three spatial dimensions are provided. Finally, concluding remarks are stated in Section 7.

## 2 Scattered Data Approximation

Let  $\Omega \subseteq \mathbb{R}^d$  denote a domain, and  $\mathcal{H}$  Hilbert space of functions mapping  $\Omega$  to  $\mathbb{R}$ . If  $\mathcal{H} \subseteq C(\Omega)$ , then  $\mathcal{H}$  is a *reproducing kernel Hilbert space* (RKHS) and there exists a unique *reproducing kernel*  $K: \Omega \times \Omega \rightarrow \mathbb{R}$  such that  $K(\cdot, \mathbf{x}) \in \mathcal{H}$  for all  $\mathbf{x} \in \Omega$  and each element  $f \in \mathcal{H}$  can be point-wise recovered, i.e.,  $f(\mathbf{x}) = \langle f, K(\cdot, \mathbf{x}) \rangle_{\mathcal{H}}$ . It is well-known, see, e.g. [46], that reproducing kernels are symmetric and *positive semi-definite*, i.e., the kernel matrix  $\mathbf{A} = [K(\mathbf{x}_i, \mathbf{x}_j)]_{i,j}$  is symmetric and positive semi-definite for all  $\{\mathbf{x}_1, \dots, \mathbf{x}_N\} \subseteq \Omega$  and all  $N \in \mathbb{N}$ .

In this article, we focus on kernels that are induced by *radial functions*. A function  $\Phi: \mathbb{R}^d \rightarrow \mathbb{R}$  is called radial, iff there is a function  $\phi: [0, \infty) \rightarrow \mathbb{R}$  such that  $\Phi(\mathbf{x}) = \phi(\|\mathbf{x}\|_2)$ . If the function  $\Phi$  is positive definite in the sense that the induced kernel  $K(\mathbf{x}, \mathbf{y}) := \Phi(\mathbf{x} - \mathbf{y})$  is positive definite, then it gives rise to a reproducing kernel.

One of the most popular of these radial functions is known as *Matérn kernel* or *Sobolev spline*  $\Phi_\nu: \mathbb{R}^d \rightarrow \mathbb{R}$ , dependent on the *smoothness parameter*  $\nu > d/2$ . It is defined by

$$\phi_\nu(r) = \frac{2^{1-\nu}}{\Gamma(\nu)} r^{\nu-\frac{d}{2}} K_{\nu-\frac{d}{2}}(r), \quad r \geq 0, \quad (1)$$

where  $\Gamma$  is the Riemannian Gamma function and  $K_\beta$  is the modified Bessel function of the second kind, see [34] for example. For specific values of the smoothness parameter  $\nu$  the representation of  $\phi_\nu$  simplifies significantly, we give a selection of specific representations in Table 1.

$\nu$	$\phi_\nu(r)$	smoothness
1/2	$\exp(-r)$	$C^0$
3/2	$(1+r)\exp(-r)$	$C^2$
5/2	$(3+3r+r^2)\exp(-r)$	$C^4$
$\infty$	$\exp(-r^2)$	$C^\infty$

Table 1: Examples for different smoothness parameters  $\nu$  of the Matérn kernel.

It is well-known that the Fourier transform of  $\Phi_\nu$  decays algebraically, i.e., there holds

$$\widehat{\Phi}_\nu(\boldsymbol{\omega}) = (1 + \|\boldsymbol{\omega}\|_2^2)^{-\nu - \frac{d}{2}}, \quad \boldsymbol{\omega} \in \mathbb{R}^d,$$

see [46, Theorem 6.13] for example. This means in particular, see, e.g., [46], that  $\Phi_\nu$  is the reproducing kernel of the Sobolev-Hilbert space  $H^{\nu - \frac{d}{2}}(\mathbb{R}^d)$ . Especially, the kernel defines a pseudo-differential operator on  $\mathbb{R}^d$ , a fact which we will exploit later on.

Having fixed the kernel of interest, we now describe the problem of function approximation. We are interested in recovering an unknown function  $f \in \mathcal{H}$ , where we are given only a finite set of data  $\{(\mathbf{x}_N, f_N), \dots, (\mathbf{x}_N, f_N)\} \subset \Omega \times \mathbb{R}$ . We collect the abscissae  $\mathbf{x}_i$  in a *set of data sites*  $X := \{\mathbf{x}_1, \dots, \mathbf{x}_N\} \subset \Omega$ . Associated to this set are two characteristic quantities: the *fill distance*

$$h_{X,\Omega} := \sup_{\mathbf{x} \in \Omega} \min_{\mathbf{x}_i \in X} \|\mathbf{x} - \mathbf{x}_i\|_2$$

and the *separation radius*

$$q_X := \frac{1}{2} \min_{i \neq j} \|\mathbf{x}_i - \mathbf{x}_j\|_2.$$

For the theoretical results we present later, we require that the set of data sites is *quasi-uniform*, i.e., that there is a constant  $c_{\text{qu}} > 0$  such that

$$q_X \leq h_{X,\Omega} \leq c_{\text{qu}} q_X.$$

An easy comparison of volumes then yields, that there are constants  $c_1$  and  $c_2$  such that

$$c_1 N^{-\frac{1}{d}} \leq h_{X,\Omega} \leq c_2 N^{-\frac{1}{d}},$$

see, e.g., [46, Proposition 14.1]. Clearly, a similar estimate holds for the separation radius, too.

To recover the unknown function, we look at two approximation methods, *interpolation* and, more generally, *regularized least squares approximation* or *kernel ridge regression*. Both can be seen as finding the minimizer of the functional  $J_\lambda$  within the subspace

$$\mathcal{H}_X := \text{span}\{K(\cdot, \mathbf{x}_1), \dots, K(\cdot, \mathbf{x}_N)\}$$

spanned by the *basis of kernel translates* within an RKHS  $\mathcal{H}$ .

$$J_\lambda(s) := \sum_{i=1}^N |f_i - s(\mathbf{x}_i)|^2 + \lambda \|s\|_{\mathcal{H}}^2, \quad s \in \mathcal{H}_X,$$

where  $\lambda \geq 0$  is a *regularization parameter*. If we set  $\lambda = 0$  we force interpolation, i.e., the minimizer  $s_f := s_0^*$  of  $J_0$  satisfies  $s_f(\mathbf{x}_i) = f_i$ , for  $i = 1 \dots, N$ . This should only be chosen if we deal with no noise on the data, that is, if it holds  $f_i = f(\mathbf{x}_i)$ . In this case, the minimizer  $s_f$  coincides with the orthogonal projection of  $f$  onto  $\mathcal{H}_X$ , since there holds  $\langle f - s_f, v \rangle_{\mathcal{H}} = 0$  for any  $v \in \mathcal{H}_X$  by the reproducing property.

In any other case, one should use  $\lambda > 0$ . Even so, the numerical procedure is the same, stated in the next theorem, which is a version of the *representer theorem*, see, e.g., [43].

**Theorem 2.1.** Let  $\Omega \subseteq \mathbb{R}^d$  be a domain. Let  $K$  be the reproducing kernel of an RKHS  $\mathcal{H}$  on  $\Omega$  and  $X = \{\mathbf{x}_1, \dots, \mathbf{x}_N\} \subseteq \Omega$  be a set of sites. Then, for all  $\lambda \geq 0$ , there exists a unique solution  $s_\lambda^*$  of  $\min J_\lambda(s)$ . In addition, there exists a coefficient vector  $\boldsymbol{\alpha} \in \mathbb{R}^N$  such that

$$s_\lambda^* = \sum_{j=1}^N \alpha_j K(\cdot, \mathbf{x}_j),$$

i.e.,  $s_\lambda^* \in \mathcal{H}_X$ . Furthermore,  $\boldsymbol{\alpha}$  is the unique solution of the linear system

$$(\mathbf{A} + \lambda \mathbf{I})\boldsymbol{\alpha} = \mathbf{f}, \quad (2)$$

where  $\mathbf{A} = [K(\mathbf{x}_i, \mathbf{x}_j)]_{i,j} \in \mathbb{R}^{N \times N}$  is the kernel matrix,  $\mathbf{I} \in \mathbb{R}^{N \times N}$  is the identity matrix, and  $\mathbf{f} = [f_i] \in \mathbb{R}^N$  is the data vector.

### 3 Other Bases for $\mathcal{H}_X$

By definition of the approximation space,  $\mathcal{H}_X$  is the linear span of the basis of kernel translates. However, this might not be the most practical basis. For example, it is well-known that there is a *Lagrange basis*  $\{\chi_j\}$  satisfying  $\chi_j(\mathbf{x}_i) = \delta_{i,j}$ ,  $i, j = 1 \dots, N$ . The Lagrange basis is well-understood and we refer to the vast amount of available literature, see [20, 12, 10, 46] and the references therein. Another basis is the *Newton basis*, which amounts to an orthogonal basis of  $\mathcal{H}_X$ , compare [35, 36]. The general concept of *dual pairs* is introduced in Section 3.1. We repeat some important properties in Section 3.2 and give an alternative proof of the exponential decay property by interpreting the underlying operators as *pseudo-differential operators*. This view, although well-established in the theory of partial differential equation, is new in the context of approximation theory.

#### 3.1 Dual Pairs

A *dual pair*  $\{(\phi_i, \tilde{\phi}_i)\}$  is a set of pairs of basis functions for  $\mathcal{H}_X$  such that  $\langle \phi_i, \tilde{\phi}_j \rangle_{\mathcal{H}} = \delta_{i,j}$  for all  $i, j = 1, \dots, N$ . Thus, we immediately obtain the representations

$$s_f = \sum_{i=1}^N \langle f, \tilde{\phi}_i \rangle_{\mathcal{H}} \phi_i = \sum_{i=1}^N \langle f, \phi_i \rangle_{\mathcal{H}} \tilde{\phi}_i$$

for the sought kernel interpolant. Its computation can therefore be accelerated if the basis functions under consideration admit sparse representations.

Obviously, the kernel matrix

$$\mathbf{A} = [K(\mathbf{x}_i, \mathbf{x}_j)]_{i,j=1}^N = [\langle K(\cdot, \mathbf{x}_i), K(\cdot, \mathbf{x}_j) \rangle_{\mathcal{H}}]_{i,j=1}^N$$

is the Gramian of basis of kernel translates. Hence, any choice of  $\gamma \in \mathbb{R}$  yields a dual pair by defining

$$[\tilde{\phi}_1, \dots, \tilde{\phi}_N] = \mathbf{k}(\cdot) \mathbf{A}^{-1-\gamma} \quad \text{and} \quad [\phi_1, \dots, \phi_N] = \mathbf{k}(\cdot) \mathbf{A}^\gamma,$$

where we set

$$\mathbf{k}(\mathbf{x}) = [K(\cdot, \mathbf{x}_1), \dots, K(\cdot, \mathbf{x}_N)].$$

Canonical choices are  $\gamma = 0$ , yielding the *Lagrange basis*, and  $\gamma = -1/2$ , yielding an orthogonal basis, where we have  $\phi_i = \tilde{\phi}_i$  for all  $i = 1, \dots, N$ . Furthermore, we notice that we have

$$\mathbf{A}^{-1} = \mathbf{A}^{-1/2} \mathbf{A}^{-1/2} = \mathbf{L} \mathbf{L}^\top,$$

where  $\mathbf{L}$  is the Cholesky factor of  $\mathbf{A}^{-1}$ . Hence, there exists an isometry such that  $\mathbf{L} = \mathbf{Q} \mathbf{A}^{-1/2}$ , which implies that another orthonormal basis of the space  $\mathcal{H}_X$  is obtained by the Cholesky decomposition of  $\mathbf{A}^{-1}$ . It is called *Newton basis* in literature, since the  $i$ -th basis function has  $i$  zeros, compare [35, 36].



### 3.2 About the Lagrange Basis

We shall first collect some results for the Lagrange basis. Since the basis elements  $\chi_i$  are elements of  $\mathcal{H}_X$ , we can express them as

$$\chi_i = \sum_{k=1}^N \alpha_k^{(i)} K(\cdot, \mathbf{x}_k), \quad i = 1, \dots, N,$$

for certain coefficient vectors  $\boldsymbol{\alpha}^{(i)} \in \mathbb{R}^N$  for any  $i = 1, \dots, N$ . There are different ways to compute these coefficient vectors. We consider two of them.

The first one allows us to compute these vectors a-priori in an offline phase, as soon as the set of data sites is fixed. The Lagrange condition  $\chi_j(\mathbf{x}_i) = \delta_{i,j}$  directly leads to the linear system

$$\mathbf{A}\boldsymbol{\alpha}^{(i)} = \mathbf{e}_i$$

for the  $i$ -th coefficient vector, where  $\mathbf{A} = [K(\mathbf{x}_i, \mathbf{x}_j)]_{i,j}$  is again the kernel matrix and  $\mathbf{e}_i \in \mathbb{R}^N$  is the  $i$ -th unit vector.

With the second method we can compute all  $\chi_i(\mathbf{x})$ , i.e., the Lagrange basis evaluated in a  $\mathbf{x} \in \mathbb{R}^d$ , simultaneously, by solving the linear system

$$[\chi_1(\mathbf{x}), \dots, \chi_N(\mathbf{x})]\mathbf{A} = \mathbf{k}(\mathbf{x}),$$

which has a unique solution for every  $\mathbf{x} \in \mathbb{R}^d$ . This leads to the representation

$$\chi_i(\mathbf{x}) = \sum_{j=1}^N [\mathbf{A}^{-1}]_{i,j} K(\mathbf{x}, \mathbf{x}_j) \quad (3)$$

$$= \mathbf{k}(\mathbf{x})\mathbf{A}^{-1}\mathbf{e}_i, \quad i = 1, \dots, N. \quad (4)$$

With the Lagrange functions at hand, we can represent the minimizer  $s_f$  of  $J_0$  by

$$s_f(\mathbf{x}) = \sum_{i=1}^N f(\mathbf{x}_i)\chi_i(\mathbf{x}). \quad (5)$$

Often, this representation is associated with a *quasi-interpolation process*, see, e.g., [7], however, in the context of this paper, we do not expect to have polynomial reproduction, a property commonly expected of quasi-interpolation.

Motivated by the desire to obtain a similar representation for  $s_\lambda^*$  with  $\lambda > 0$ , we define the *modified Lagrange basis* via

$$\chi_{\lambda,i}(\mathbf{x}) = \sum_{j=1}^N [\mathbf{A} + \lambda\mathbf{I}]_{i,j}^{-1} K(\mathbf{x}, \mathbf{x}_j) \quad (6)$$

$$= \mathbf{k}(\mathbf{x})(\mathbf{A} + \lambda\mathbf{I})^{-1}\mathbf{e}_i, \quad i = 1, \dots, N. \quad (7)$$

Employing the modified Lagrange basis, we can represent  $s_\lambda^*$  as

$$s_\lambda^*(\mathbf{x}) = \sum_{i=1}^N f_i \chi_{\lambda,i}(\mathbf{x}). \quad (8)$$

For the Matérn kernel  $K(\mathbf{x}, \mathbf{y}) = \Phi_\nu(\mathbf{x} - \mathbf{y})$ , it turns out that the dual basis associated to the basis of kernel translates, i.e., the Lagrange basis, is highly localized, that is,  $|\chi_i(\mathbf{x})|$  decays exponentially fast if  $\|\mathbf{x} - \mathbf{x}_i\|_2$  grows. This is a direct consequence of the fact that the entries of the inverse of the kernel matrix  $\mathbf{A}$  exhibit an exponential off-diagonal decay. These can be quantified as follows.

**Corollary 3.1.** *Let  $X = \{\mathbf{x}_1, \dots, \mathbf{x}_N\}$  be a quasi-uniform set of sites with fill distance  $h_{X,\Omega} < h_0$  and separation radius  $q_X$ . Let  $\Phi_\nu$  be the Matérn kernel with smoothness parameter*

$\nu$ , such that  $\nu - d/2 \in \mathbb{N}$ . Then there is a constant  $C > 0$  such that the entries of the inverse of the kernel matrix satisfy the estimate

$$|[\mathbf{A}^{-1}]_{j,k}| \leq C q_X^{d-2\nu} \exp\left(-\eta \frac{\|\mathbf{x}_j - \mathbf{x}_k\|_2}{h_{X,\Omega}}\right), \quad (9)$$

where  $\eta = \eta(\nu, d) < 1$  is a positive constant. This implies the following decay condition on the Lagrange basis

$$|\chi_i(\mathbf{x})| \leq C \left(\frac{h_{X,\Omega}}{q_X}\right)^{\nu - \frac{d}{2}} \exp\left(-\mu \frac{\|\mathbf{x} - \mathbf{x}_i\|_2}{h_{X,\Omega}}\right), \quad \mathbf{x} \in \mathbb{R}^d, \text{ for } i = 1, \dots, N,$$

with  $\mu = -\frac{h_0}{4} \log(\eta)$ .

The first proofs of this corollary were given in [12] for  $\Omega = \mathbb{S}^{d-1}$ , the  $d - 1$  dimensional sphere. In [20], it was refined to the version given here for general bounded domains. In the next subsection, we offer an alternative proof by considering the kernel in the context of pseudo-differential operators.

We see in (4) and (7) that the main computational task to evaluate the (modified) Lagrange basis  $\{\chi_i\}$  and  $\{\chi_{\lambda,i}\}$ , respectively, is the inversion of the dense, positive definite matrix  $\mathbf{A}$  or  $\mathbf{A} + \lambda \mathbf{I}$ , respectively, whose entries decay exponentially apart from the diagonal. Hence, the desired fast evaluation of the approximation  $s_\lambda^*$  can be achieved by finding efficient ways to approximate the kernel matrix  $\mathbf{A}$  and its inverse  $\mathbf{A}^{-1}$ .

### 3.3 Alternative Point of View: Pseudo-differential Operators

In this subsection, let  $\Omega \subset \mathbb{R}^d$  be a smooth domain. Then, the reproducing kernel under consideration gives rise to a compact integral operator on  $L^2(\Omega)$  according to

$$\mathcal{K} : L^2(\Omega) \rightarrow L^2(\Omega), \quad u \mapsto \int_{\Omega} K(\cdot, \mathbf{y}) u(\mathbf{y}) d\mathbf{y}. \quad (10)$$

For many kernel functions,  $\mathcal{K}$  constitutes a classical pseudo-differential operator of negative order  $s < 0$ . We refer to e.g. [25, 37, 42, 45] for the details of this theory, including the subsequent developments.

We are especially interested in pseudo-differential operators  $\mathcal{K}$  which belong to the subclass  $OPS_{cl,1}^s$  of *analytic* pseudo-differential operators, see [37]. Their kernels are known to be *asymptotically smooth*, meaning that there holds the decay property

$$\forall \boldsymbol{\alpha}, \boldsymbol{\beta} \in \mathbb{N}^d : \exists \rho > 0 : \quad |\partial_{\mathbf{x}}^{\boldsymbol{\alpha}} \partial_{\mathbf{y}}^{\boldsymbol{\beta}} K(\mathbf{x}, \mathbf{y})| \leq C \frac{(|\boldsymbol{\alpha}| + |\boldsymbol{\beta}|)!}{(\rho \|\mathbf{x} - \mathbf{y}\|_2^{s+d})^{|\boldsymbol{\alpha}| + |\boldsymbol{\beta}|}}, \quad (\mathbf{x}, \mathbf{y}) \in (\Omega \times \Omega) \setminus \Delta \quad (11)$$

apart from the diagonal  $\Delta := \{(\mathbf{x}, \mathbf{y}) \in \Omega \times \Omega : \mathbf{x} = \mathbf{y}\}$  for some constant  $C > 0$ . This estimate is the key for the computational treatment of the underlying kernel matrices by means of hierarchical matrix techniques [15] or wavelet matrix compression [5, 9].

A special feature of pseudo-differential operators is that they form an algebra, which we can be exploited for kernel matrices. Besides addition, the concatenation of two pseudo-differential operators  $\mathcal{K}$  and  $\mathcal{K}'$  essentially corresponds to the product of the respective kernel matrices  $\mathbf{A}$  and  $\mathbf{B}$  under the assumption that the set of data sites is asymptotically uniformly distributed modulo one. This means, we have for every Riemann integrable function  $f : \Omega \rightarrow \mathbb{R}$  that

$$\left| \int_{\Omega} f(\mathbf{x}) d\mathbf{x} - \frac{|\Omega|}{N} \sum_{i=1}^N f(\mathbf{x}_i) \right| \rightarrow 0 \quad \text{as } N \rightarrow \infty,$$

compare [30]. Under this assumption, the concatenation  $\mathcal{K} \circ \mathcal{K}'$  corresponds to the matrix-matrix product  $\mathbf{AB}$ . Indeed, the kernel  $K''$  of the concatenated pseudo-differential operator satisfies

$$K''(\mathbf{x}_i, \mathbf{x}_j) = \int_{\Omega} K(\mathbf{x}_i, \mathbf{z}) K'(\mathbf{z}, \mathbf{x}_j) d\mathbf{z} \approx \frac{|\Omega|}{N} \sum_{k=1}^N K(\mathbf{x}_i, \mathbf{x}_k) K'(\mathbf{x}_k, \mathbf{x}_j) = [\mathbf{A}]_{i,:} [\mathbf{B}]_{:,j}.$$

This means that the matrix  $\mathbf{AB}$  approximates the kernel matrix induced by  $K''$ . As this is a compressible pseudo-differential operator,  $\mathbf{AB}$  is also compressible, compare [23, Theorem 4]. This property can be used to show that the inverse kernel matrix is compressible.

Consider a symmetric and positive definite kernel  $K$  such that the associated pseudo-differential operator satisfies  $\mathcal{K} \in OPS_{cl,1}^s$  with  $s < 0$ . Then, the inverse of  $\mathcal{K} + \lambda I$  is of the form  $\lambda^{-1}I - \mathcal{K}'$  with  $\mathcal{K}'$  being likewise a pseudo-differential operator from  $OPS_{cl,1}^s$ , see [23, Lemma 2]. Especially, the Schwarz kernel  $K'$  which underlies the operator  $\mathcal{K}'$  by the Schwartz kernel theorem, see, e.g., [26, Chap. 5], is symmetric, positive definite, and likewise asymptotically smooth. Thus, the inverse of a (regularized) kernel matrix is compressible in view of the above mentioned link between the matrix-matrix product and the concatenation of the associated pseudo-differential operators.

We like to mention that the theory of pseudo-differential operators is a theoretical foundation for the observations made already earlier. Indeed, it has been observed that the inverse of a kernel matrix is compressible, compare for example [14, 16] and more recently [2] in case of  $\mathcal{H}$ -matrices and [4, 40] for the case of wavelet matrix compression. Especially, in the case of the Matérn kernel, the associated pseudo-differential operator corresponds to a Bessel potential operator. The symbol of the Matérn kernel is  $(1 + \|\xi\|^2)^{d/2-\nu}$ , which implies that the inverse pseudo-differential operator has the symbol  $(1 + \|\xi\|^2)^{\nu-d/2}$ . In case of  $\nu = 1/2, 3/2, \dots$ , this represents a differential operator and hence a local operator. This explains the exponential decay (9) of the inverse to the kernel matrix in this case, see also [38]. Note that, the symbol is an analytic function in  $r = \|\xi\|$  for  $\nu \neq 1/2, 3/2, \dots$ , hence the Schwartz kernel of the inverse kernel matrix still decreases rapidly as  $r \rightarrow \infty$ . We should finally mention that one may weaken the strong assumptions on the kernels under consideration, if the Gevrey extension of the symbolic calculus for classical pseudo-differential operators is used as developed in [6, 29, 37].

## 4 Efficient Computation of the Lagrange Basis

We now turn to introducing a framework to efficiently compute the Lagrange basis. As already discussed above and quantified in Corollary 3.1, the kernel matrix of the Matérn kernel and more generally kernels of pseudo-differential operators exhibit a fast off-diagonal decay. The authors of [20, 12, 19] used this fact to derive localizations of the Lagrange basis. First, we review the basic ideas of their approach and use them afterwards to derive symmetric and sparse preconditioners for the notoriously ill conditioned kernel matrix.

### 4.1 Cut-off and Localized Lagrange Functions

In the case of the Matérn kernel, we can exploit the exponential decay in (9) and either ignore coefficients in the expansions (3) and (6), respectively, that are smaller than a given threshold or directly construct functions that satisfy the Lagrange condition only on a small neighborhood of  $\mathbf{x}_i \in X$ . The resulting functions are called *cut-off Lagrange basis* and *localized Lagrange basis*, respectively. We now go into more detail.

Motivated by (9), we define the *footprint*  $X_i$  of the  $i$ -th Lagrange basis element as

$$X_i = \{\mathbf{x}_j \in X : \|\mathbf{x}_i - \mathbf{x}_j\|_2 \leq \kappa h_{X,\Omega} |\log(h_{X,\Omega})|\}, \quad (12)$$

with a free constant  $\kappa > 0$ , independent of  $i$ . Then, the cut-off Lagrange basis element  $\chi_i^{\text{co}}$  is given as

$$\chi_i^{\text{co}}(\mathbf{x}) = \sum_{j: \mathbf{x}_j \in X_i} [\mathbf{A}^{-1}]_{i,j} K(\mathbf{x}, \mathbf{x}_j).$$

Analogously, we have

$$\chi_{\lambda,i}^{\text{co}}(\mathbf{x}) = \sum_{j: \mathbf{x}_j \in X_i} [(\mathbf{A} + \lambda \mathbf{I})^{-1}]_{i,j} K(\mathbf{x}, \mathbf{x}_j), \quad (13)$$

for the modified cut-off Lagrange basis. Note that we only changed the number of indices entering the summation and kept the coefficients in the expansion the same as in the full Lagrange basis.

The idea of the localized Lagrange basis is now to enforce the Lagrange condition only on the footprint, i.e., we define the basis elements  $\chi_i^{\text{loc}}$  and  $\chi_{\lambda,i}^{\text{loc}}$  as

$$\chi_i^{\text{loc}} := \sum_{j: \mathbf{x}_j \in X_i} \alpha_j^{(i)} K(\cdot, \mathbf{x}_j), \quad \text{and} \quad \chi_{\lambda,i}^{\text{loc}} := \sum_{j: \mathbf{x}_j \in X_i} \beta_j^{(i)} K(\cdot, \mathbf{x}_j)$$

where the coefficient vectors  $\boldsymbol{\alpha}^{(i)}, \boldsymbol{\beta}^{(i)} \in \mathbb{R}^{|X_i|}$  are the respective unique solutions of the linear systems

$$\mathbf{A}|_{X_i} \boldsymbol{\alpha}^{(i)} = \mathbf{e}_m \quad \text{and} \quad (\mathbf{A}|_{X_i} + \lambda \mathbf{I}) \boldsymbol{\beta}^{(i)} = \mathbf{e}_m \quad (14)$$

with  $\mathbf{A}|_{X_i} = [K(\mathbf{x}_j, \mathbf{x}_\ell)]_{\mathbf{x}_j, \mathbf{x}_\ell \in X_i}$  being the restriction of the kernel matrix  $\mathbf{A}$  to indices in  $X_i$  and  $\mathbf{e}_m \in \mathbb{R}^{|X_i|}$  being the unit vector whose 1-entry is in the (local) coordinate  $m \in \{1, \dots, |X_i|\}$  that relates to the (global) coordinate  $i \in \{1, \dots, N\}$ .

While the cut-off Lagrange basis still requires to assemble the full kernel matrix we can achieve faster evaluation of the approximation  $s_\lambda^{*,\text{co}}$ . The localized Lagrange basis, on the other hand, reduces the computational cost since we have to solve for every  $i = 1, \dots, N$  a linear system of the size  $|X_i| \times |X_i|$ . Hence, if the number of points in the footprints is sufficiently small, this is cheaper than the cost to compute the full or cut-off Lagrange basis.

Following the representations of the interpolant or penalized least-squares approximation in (5) and (8), respectively, we can use the cut-off and localized Lagrange functions to derive representations of approximations

$$s_f^{\text{co}} = \sum_{i=1}^N f(\mathbf{x}_i) \chi_i^{\text{co}} \quad \text{and} \quad s_\lambda^{*,\text{co}} = \sum_{i=1}^N f_i \chi_{\lambda,i}^{\text{co}} \quad (15)$$

or

$$s_f^{\text{loc}} = \sum_{i=1}^N f(\mathbf{x}_i) \chi_i^{\text{loc}} \quad \text{and} \quad s_\lambda^{*,\text{loc}} = \sum_{i=1}^N f_i \chi_{\lambda,i}^{\text{loc}}. \quad (16)$$

For the localized Lagrange basis, the following estimate is known, see [18]. Clearly, this translates immediately into an estimate for the difference  $s_f - s_f^{\text{loc}}$ .

**Proposition 4.1.** *With the notation and assumptions of Corollary 3.1, where  $m := \nu - d/2 \in \mathbb{N}$ , let the Lagrange basis element  $\chi_i$  be defined as in (3) and the localized Lagrange basis element  $\chi_i^{\text{loc}}$  be defined as in (13) with footprint (12). Then there exists a constant  $C > 0$  such that the error estimate*

$$\|\chi_i - \chi_i^{\text{loc}}\|_{W_p^\sigma(\mathbb{R}^d)} \leq C h_{X,\Omega}^{\frac{\kappa}{2} + d - 2m}, \quad i = 1, \dots, N,$$

holds for  $1 \leq p \leq \infty$  and  $\sigma < 2m - d + \frac{d}{p}$ .

We now want to discuss the cost of computing the localized Lagrange basis. Since we assume that the set of data sites  $X$  is quasi-uniform, we can bound the number of points in the footprint  $X_i$ , independently of  $i$ , by

$$|X_i| \leq C \left( \frac{\kappa}{d} \log N \right)^d \quad (17)$$

with a constant  $C > 0$ , independent of  $N$ , if  $\frac{\kappa}{d} \log N > 1$ .

Hence, we have to solve  $N$  dense linear systems of size  $\mathcal{O}((\log^d N) \times (\log^d N))$ . This means, a naive ansatz, i.e., not using any further properties the local matrices exhibit, computes the coefficients for the localized Lagrange basis with cost  $\mathcal{O}(N \log^{3d} N)$ . However, we emphasize that the systems are all independent of each other, which makes it possible to efficiently parallelize the computation. Further, we note that we only need to keep  $\mathcal{O}(N \log^d N)$  coefficients in memory, compared to the  $\mathcal{O}(N^2)$  coefficients for the full Lagrange basis. This means, from a different point of view, we find an elegant compression of the inverse of the kernel matrix  $\mathbf{A}$ .

## 4.2 Symmetrized Version for Preconditioning

A drawback of the construction in Section 4.1 is that it is non-symmetric in the following sense. Collecting the column vectors  $\boldsymbol{\alpha}^{(i)}$  and  $\boldsymbol{\beta}^{(i)}$  for all  $i = 1, \dots, N$  in a global matrix  $\mathbf{B}$  yields a (sparse) matrix that satisfies  $\mathbf{A}\mathbf{B} \approx \mathbf{I}$  or  $(\mathbf{A} + \lambda\mathbf{I})\mathbf{B} \approx \mathbf{I}$ , respectively. Nonetheless, there holds  $\mathbf{B} \neq \mathbf{B}^T$  although we have  $\mathbf{A} = \mathbf{A}^T$ . This rules out the use of  $\mathbf{B}$  as a preconditioner in the conjugate gradient method [24]. Indeed, in [12] for example, only the generalized minimal residual method [39] has been used which, however, is much more expensive compared to the conjugate gradient method.

We shall modify the construction in (14). The matrix  $\mathbf{A}$  is symmetric and positive definite, so is the footprint matrix  $\mathbf{A}|_{X_i}$  for any subset  $X_i \subset X$ . Therefore, the first possibility we have is to use the matrix square root  $\mathbf{A}|_{X_i}^{1/2}$  of the footprint matrix. Then, we solve in complete analogy to (14) the systems

$$\mathbf{A}|_{X_i}^{1/2} \tilde{\boldsymbol{\alpha}}^{(i)} = \mathbf{e}_m \quad (18)$$

for all  $i = 1, \dots, N$ . Likewise to above, we then form a (sparse) matrix  $\mathbf{C}$  from all of the column vectors  $\tilde{\boldsymbol{\alpha}}^{(i)}$ ,  $1 \leq j \leq N$ , which satisfies  $\mathbf{A}^{1/2}\mathbf{C} \approx \mathbf{I}$  and hence  $\mathbf{C}^T\mathbf{A}^{1/2} \approx \mathbf{I}$ . Thus, we also conclude  $\mathbf{C}^T\mathbf{A}\mathbf{C} \approx \mathbf{I}$  and  $\mathbf{C}\mathbf{C}^T$  defines a symmetric and positive definite preconditioner for  $\mathbf{A}$ .

Alternatively, we can also use the Cholesky decomposition  $\mathbf{A}|_{X_i} = \mathbf{L}_i\mathbf{L}_i^T$  of size  $|X_i| \times |X_i|$  of the kernel matrix restricted to the footprints, solving the systems

$$\mathbf{L}_i^T \tilde{\boldsymbol{\alpha}}^{(i)} = \mathbf{e}_m$$

for all  $i = 1, \dots, N$ . If we then form the (sparse) matrix  $\mathbf{C}$  from all of the column vectors  $\tilde{\boldsymbol{\alpha}}^{(i)}$ ,  $i = 1, \dots, N$ , then there holds  $\mathbf{L}^T\mathbf{C} \approx \mathbf{I}$  and hence  $\mathbf{C}^T\mathbf{L} \approx \mathbf{I}$ , where  $\mathbf{L}\mathbf{L}^T = \mathbf{A}$  is the Cholesky decomposition of  $\mathbf{A}$ . Consequently,  $\mathbf{C}^T\mathbf{L}\mathbf{L}^T\mathbf{C} \approx \mathbf{I}$  and  $\mathbf{C}\mathbf{C}^T$  defines likewise a symmetric and positive definite preconditioner for  $\mathbf{A}$ .

In case of the original footprint systems (14) and in case of the matrix square root (18), the ordering of the local indices  $X_i$  does not affect the so constructed global matrices  $\mathbf{B}$  and  $\mathbf{C}$ , respectively. The reason for this is that the solution vectors  $\boldsymbol{\alpha}^{(i)}$  and  $\tilde{\boldsymbol{\alpha}}^{(i)}$ , respectively, are then just permuted versions of the same vectors. This is completely different in case of the Cholesky decomposition. Only in the case of an ordering of the local indices which respects the ordering of the global ones,  $\mathbf{C}$  is an upper triangular matrix since each vector  $\tilde{\boldsymbol{\alpha}}^{(i)}$  has zero entries for all indices being larger than the respective local index  $m$ . In this case, we have hence constructed a localized *Newton basis*, compare [36].

In complete analogy, we can also address the regularized kernel matrices

$$(\mathbf{A} + \lambda\mathbf{I})|_{X_i}^{1/2} \tilde{\boldsymbol{\beta}}^{(i)} = \mathbf{e}_m \quad \text{or} \quad \mathbf{L}_j^T \tilde{\boldsymbol{\beta}}^{(i)} = \mathbf{e}_m,$$

where  $\mathbf{L}_i\mathbf{L}_i^T$  is the Cholesky decomposition of the regularized kernel matrix  $\mathbf{A}|_{X_i} + \lambda\mathbf{I}$ . This yields a symmetric and positive definite preconditioner for  $\mathbf{A} + \lambda\mathbf{I}$ . We should finally mention that the computation of the matrix  $\mathbf{C}\mathbf{C}^T$  should be avoided, meaning that the matrix-vector multiplication  $\mathbf{z} = \mathbf{C}\mathbf{C}^T\mathbf{x}$  is computed in two steps in accordance with  $\mathbf{y} = \mathbf{C}^T\mathbf{x}$  and  $\mathbf{z} = \mathbf{C}\mathbf{y}$ .

In order to give a visual idea the of basis of kernel translates, the corresponding Lagrange basis and the orthogonal basis obtained from the inverse square root of the kernel matrix  $\mathbf{A}$ , we consider the Sobolev space  $H^1(\mathbb{R})$ , equipped with the usual norm

$$\|u\|_{H^1(\mathbb{R})}^2 = \|u\|_{L^2(\mathbb{R})}^2 + \|u'\|_{L^2(\mathbb{R})}^2.$$

Its reproducing kernel is given by  $K(x, y) = \frac{1}{2} \exp(-|x - y|)$ , see [46] for instance. Fig. 1 shows different basis elements and the corresponding Lagrange basis elements. The bottom row shows the associated orthonormal basis, each for  $N = 200$  equidistant data sites in  $[-1, 1]$ .

## 5 Dual Pairs in Samplet Coordinates

In Section 4.1, we leveraged the exponential decay of the entries of the inverse kernel matrix (9) to construct dual pairs and quasi-interpolations to the given data and speed-up the evaluation of these. In this section, we pursue a multiresolution approach based on a samplet basis

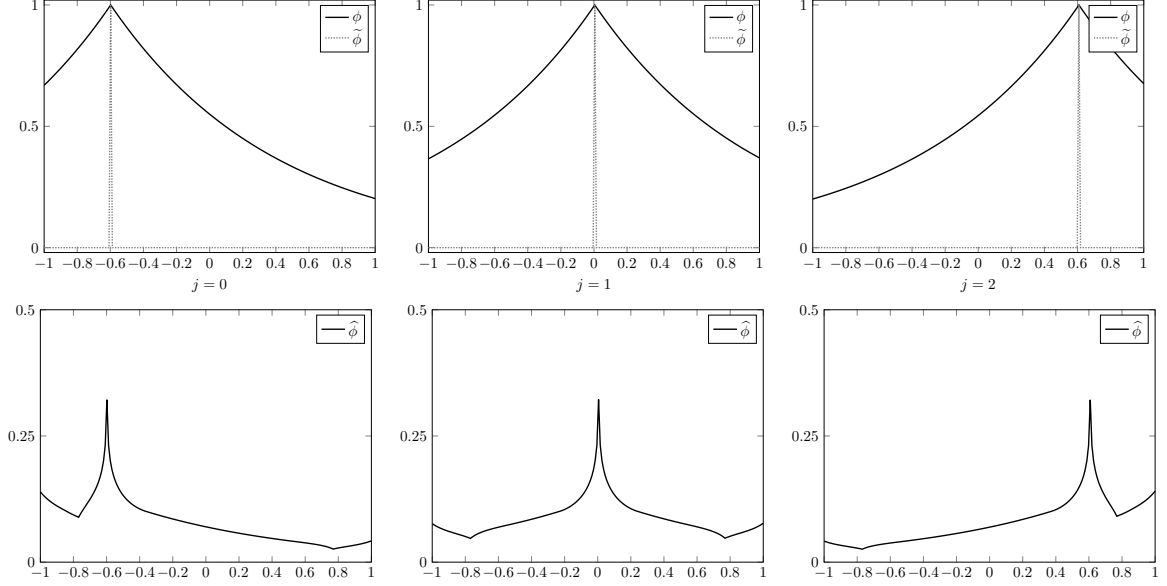


Figure 1: Basis of kernel translates, localized Lagrange basis for  $H^1(\mathbb{R})$  (top row). The bottom row shows the corresponding orthogonal functions obtained with the square root of the inverse Gramian  $\mathbf{A}^{-1/2}$ .

embedded into a reproducing kernel Hilbert space. This way, we obtain a sparse representation of the kernel matrix and a corresponding direct solver. We emphasize, however, that the resulting approximations will most likely not satisfy any Lagrange condition. Nevertheless, we will be able to define *quasi-interpolations* in the style of (15) or (16). For the reader's convenience, we start by briefly recalling the construction of a samplet basis.

## 5.1 Samplet Basis Construction

The first building block in the samplet construction is a *cluster tree* for the set  $X$ . This is a tree  $\mathcal{T}$  with root  $X$  and each node  $\tau \in \mathcal{T}$  is the disjoint union of its children. We refer to [21] for details. The cluster tree  $\mathcal{T}$  directly induces a support based hierarchical clustering of the subspace  $\mathcal{H}'_X := \text{span}\{\delta_{\mathbf{x}_1}, \dots, \delta_{\mathbf{x}_N}\} \subset \mathcal{H}'$  spanned by the Dirac- $\delta$ -distributions supported at the data sites in  $X$ . With a slight abuse of notation, we will refer to this cluster tree also by  $\mathcal{T}$  and to its elements by  $\tau$ . Based on the multilevel hierarchy generated by the cluster tree, we shall now construct a multiresolution basis for  $\mathcal{H}'_X$ . We start by introducing a *two-scale transform* between basis elements on a cluster  $\tau$  of level  $j$ . To this end, we represent scaling distributions  $\Phi_j^\tau = \{\varphi_{j,k}^\tau\}$  and samplets  $\Sigma_j^\tau = \{\sigma_{j,k}^\tau\}$  recursively as linear combinations of the scaling distributions  $\Phi_{j+1}^\tau$  of  $\tau$ 's child clusters. This amounts to the *refinement relations*

$$\varphi_{j,k}^\tau = \sum_{\ell=1}^{n_{j+1}^\tau} q_{j,\Phi,\ell,k}^\tau \varphi_{j+1,\ell}^\tau \text{ and } \sigma_{j,k}^\tau = \sum_{\ell=1}^{n_{j+1}^\tau} q_{j,\Sigma,\ell,k}^\tau \varphi_{j+1,\ell}^\tau \text{ with } n_{j+1}^\tau := |\Phi_{j+1}^\tau|,$$

which may be written in matrix notation as

$$[\Phi_j^\tau, \Sigma_j^\tau] = \Phi_{j+1}^\tau \mathbf{Q}_j^\tau = \Phi_{j+1}^\tau [\mathbf{Q}_{j,\Phi}^\tau, \mathbf{Q}_{j,\Sigma}^\tau]. \quad (19)$$

To obtain vanishing moments and orthonormality, the transform  $\mathbf{Q}_j^\tau$  is derived from an orthogonal decomposition of the *moment matrix*  $\mathbf{M}_{j+1}^\tau \in \mathbb{R}^{m_q \times n_{j+1}^\tau}$ , given by

$$\mathbf{M}_{j+1}^\tau := \begin{bmatrix} (\mathbf{x}^0, \varphi_{j+1,1})_\Omega & \cdots & (\mathbf{x}^0, \varphi_{j+1,n_{j+1}^\tau})_\Omega \\ \vdots & & \vdots \\ (\mathbf{x}^\alpha, \varphi_{j+1,1})_\Omega & \cdots & (\mathbf{x}^\alpha, \varphi_{j+1,n_{j+1}^\tau})_\Omega \end{bmatrix} = [(\mathbf{x}^\alpha, \Phi_{j+1}^\tau)_\Omega]_{|\alpha| \leq q}.$$

Herein,  $m_q = \binom{q+d}{d}$  denotes the dimension of the space  $\mathcal{P}_q(\Omega)$  of total degree polynomials.

In the original construction by Tausch and White [44], the matrix  $\mathbf{Q}_j^\tau$  is obtained from the singular value decomposition of  $\mathbf{M}_{j+1}^\tau$ . For the construction of samplers, we follow the idea from [1] and rather employ the QR decomposition, which results in samplers with an increasing number of vanishing moments. We compute

$$(\mathbf{M}_{j+1}^\tau)^\top = \mathbf{Q}_j^\tau \mathbf{R} =: [\mathbf{Q}_{j,\Phi}^\tau, \mathbf{Q}_{j,\Sigma}^\tau] \mathbf{R} \quad (20)$$

The moment matrix for the cluster's scaling distributions and samplers is now given by

$$\begin{aligned} [\mathbf{M}_{j,\Phi}^\tau, \mathbf{M}_{j,\Sigma}^\tau] &= [(\mathbf{x}^\alpha, [\Phi_j^\tau, \Sigma_j^\tau])_\Omega]_{|\alpha| \leq q} \\ &= [(\mathbf{x}^\alpha, \Phi_{j+1}^\tau [\mathbf{Q}_{j,\Phi}^\tau, \mathbf{Q}_{j,\Sigma}^\tau])_\Omega]_{|\alpha| \leq q} = \mathbf{M}_{j+1}^\tau [\mathbf{Q}_{j,\Phi}^\tau, \mathbf{Q}_{j,\Sigma}^\tau] = \mathbf{R}^\top. \end{aligned}$$

Since  $\mathbf{R}^\top$  is a lower triangular matrix, the first  $k-1$  entries in its  $k$ -th column are zero. This amounts to  $k-1$  vanishing moments for the  $k$ -th distribution generated by the orthogonal transform  $\mathbf{Q}_j^\tau = [\mathbf{Q}_{j,\Phi}^\tau, \mathbf{Q}_{j,\Sigma}^\tau]$ . Defining the first  $m_q$  distributions as scaling distributions and the remaining ones as samplers, we obtain samplers with vanishing moments at least of order  $q+1$ .

For leaf clusters, we define the scaling distributions by Dirac- $\delta$ -distributions supported at the points  $\mathbf{x}_i$ , i.e.,  $\Phi^\tau := \{\delta_{\mathbf{x}_i} : \mathbf{x}_i \in \tau, \tau \in \mathcal{L}(\mathcal{T})\}$ . The scaling distributions of all clusters on a specific level  $j$  then generate the spaces

$$\mathcal{X}_j := \text{span} \{ \varphi_{j,k}^\tau : k \in I_j^{\Phi,\tau}, \text{level}(\tau) = j \}. \quad (21)$$

In contrast, the samplers span the detail spaces

$$\mathcal{S}_j := \text{span} \{ \sigma_{j,k}^\tau : k \in I_j^{\Sigma,\tau}, \text{level}(\tau) = j \}. \quad (22)$$

Combining the scaling distributions of the root cluster with all clusters' samplers gives rise to the sampler basis

$$\Sigma := \Phi^X \cup \bigcup_{\tau \in \mathcal{T}} \Sigma^\tau. \quad (23)$$

## 5.2 Sampler Representation of the Lagrange Basis

The sampler basis introduced in the previous subsection can be represented according to

$$\sigma_{j,k} = \sum_{i=1}^N [\mathbf{T}]_{(j,k),i} \delta_{\mathbf{x}_i}, \quad k \in \nabla_j, j = 0, \dots, J, \quad (24)$$

where  $\nabla_j$  denote appropriate index sets. Here, the matrix  $\mathbf{T} \in \mathbb{R}^{N \times N}$  describes the sampler transform. It is an orthogonal matrix and can be applied with linear cost by means of the fast samplers transform, see [21, 33]. The key feature is that they have vanishing moments of order  $q+1$ , meaning that

$$|(f, \sigma_{j,k})_\Omega| \leq \sqrt{|\tau|} \left( \frac{d}{2} \right)^{q+1} \frac{\text{diam}(\tau)^{q+1}}{(q+1)!} \|f\|_{C^{q+1}(O)} \quad (25)$$

provided that  $f \in C^{q+1}(O)$ , where  $O \subset \Omega$  is any open set containing the sampler's support. Here,  $\tau$  denotes the cluster where the sampler is supported and  $|\tau|$  denotes the number of data sites contained in the cluster.

The sampler basis (24) gives rise to a multiresolution basis in  $\mathcal{H}_X$  by means of the Riesz isometry  $\mathcal{J} : \mathcal{H}' \rightarrow \mathcal{H}$  according to

$$\psi_{j,k} := \mathcal{J} \sigma_{j,k} = \sum_{i=1}^N [\mathbf{T}]_{(j,k),i} K(\cdot, \mathbf{x}_i), \quad k \in \nabla_j, j = 0, \dots, J.$$

We call these functions *embedded samplers*. The associated Lagrange basis is given by

$$\tilde{\psi}_{j,k} = \sum_{j',k'} [\mathbf{A}_\Sigma^{-1}]_{(j,k),(j',k')} \psi_{j',k'}, \quad k \in \nabla_j, j = 0, \dots, J.$$

Here, the kernel matrix  $\mathbf{A}_\Sigma \in \mathbb{R}^{N \times N}$  has to be taken in samplet coordinates, i.e., we have

$$\mathbf{A}_\Sigma := \mathbf{T} \mathbf{A} \mathbf{T}^\top. \quad (26)$$

Note that there holds

$$\langle (\Phi \mathbf{U})^\top, \tilde{\Phi} \mathbf{U} \rangle_{\mathcal{H}} = \mathbf{I}$$

for any orthogonal matrix  $\mathbf{U}$  and any dual pair  $(\Phi, \tilde{\Phi})$ . In particular, since the samplet transform  $\mathbf{T}$  is orthogonal, the basis  $\{\psi_{j,k}\}$  corresponds to the samplet transformed basis of kernel translates, while  $\{\tilde{\psi}_{j,k}\}$  is the samplet transformed Lagrange basis.

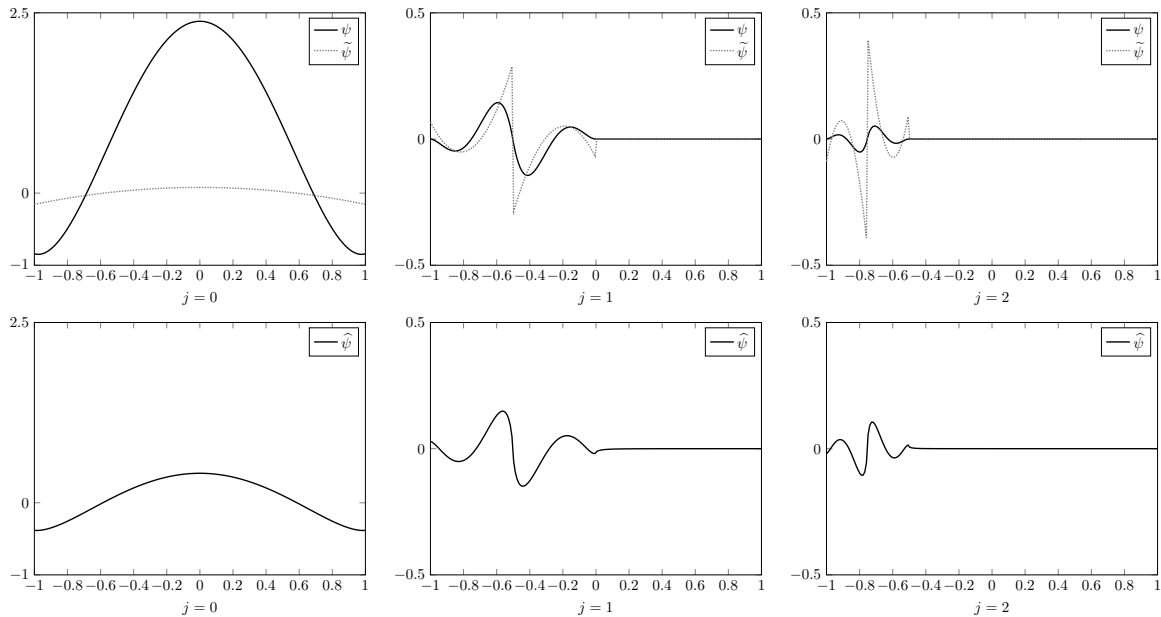


Figure 2:  $H^1(\mathbb{R})$ -embedded primal and dual scaling distribution (top left), samplet on level  $j = 1$  (top middle) and samplet on level  $j = 2$  (top right) for  $N = 200$  equidistant data sites and  $q + 1 = 3$  vanishing moments. The bottom row shows the corresponding orthogonal samplets obtained with the square root of the inverse kernel matrix  $\mathbf{A}_\Sigma^{-1/2}$ .

Similar to the single scale bases, we want to give a visual idea of the embedded samplet basis, their dual basis and the corresponding orthogonal basis. We again consider the Sobolev space  $H^1(\mathbb{R})$ . The top row of Fig. 2 shows an embedded scaling distribution (left plot) and two embedded samplets (middle and right plots) with  $q + 1 = 3$  vanishing moments, constructed for  $N = 200$  equidistant data sites. The bottom row shows the corresponding elements of the orthogonal basis obtained from the inverse square root of the inverse kernel matrix  $\mathbf{A}_\Sigma^{-1/2}$ . Different from the single scale case, the orthogonal basis remains a local basis in samplet coordinates, cp. Fig. 1.

### 5.3 Kernel Matrix Compression and Associated Algebra

Based on the asymptotic smoothness (11) of the kernel function under consideration, the kernel matrix  $\mathbf{A}$  from (26) can be compressed in samplet coordinates, such that only  $\mathcal{O}(N \log N)$  matrix entries remain, see [21]. The resulting pattern is found in the left plot of Fig. 3 for uniform random points on the unit square. According to Section 3.3, we know that the inverse kernel matrix is also compressible in samplet coordinates, using the same matrix pattern. Therefore, it remains to compute the inverse in an efficient way. One approach would be the use the Newton-Schulz iteration to compute an approximate matrix inverse, see [27, 41] for details. However, it turns out that selected inversion is much more efficient in terms of computing times, compare [23]. This issues from the fact that the samplet compressed kernel matrix can be reordered by means of nested selection [13, 32] such that the associated



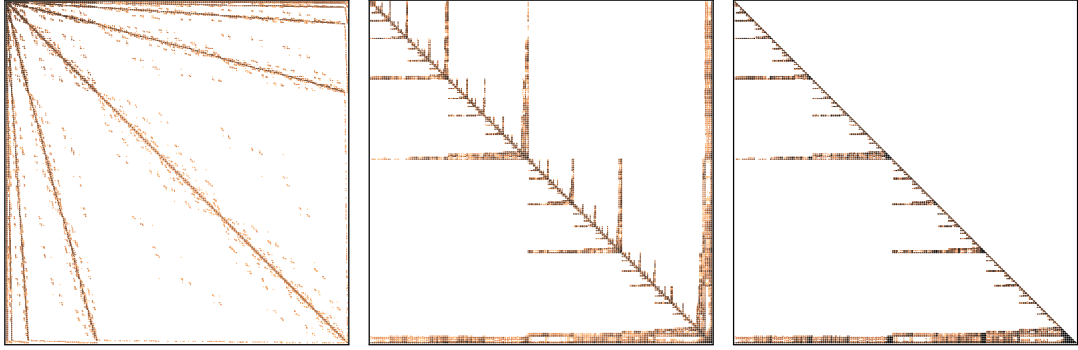


Figure 3: Typical matrix pattern of the samplet compressed kernel matrix for  $d = 2$  (left), its reordering by means of nested dissection (middle), and the associated Cholesky factor (right).

Cholesky factors have low fill-in. The reordered kernel matrix is found in the middle plot of Fig. 3 while the associated Cholesky factor is found in the right plot. In the plots, lighter blocks correspond to less entries. Selected inversion computes the inverse then based on this rather sparse Cholesky factor, see [31]. The application of the samplet compressed, inverse kernel matrix to a data vector  $\mathbf{f}$  is computable in complexity  $\mathcal{O}(N \log N)$ , independent of the data vector being given in the samplet basis or – in view of the fast samplet transform – as point evaluations.

We finally like to mention that the rapid computation of the matrix power  $\mathbf{A}^\gamma$  for  $\gamma \in \mathbb{R}$  is also possible by means of its contour integral representation [17]. We refer the reader to [23] for all the details and numerical results.

## 6 Numerical Tests

We now turn to testing the methods introduced above. Although the motivation to study the construction of the localized Lagrange and the samplet basis was to obtain dual pairs that allow faster evaluation of the quasi-interpolants, both methods can be interpreted as compression schemes of the (inverse) kernel matrix. The compression power then can be directly translated into the approximation error of the interpolant by the respective quasi-interpolants. Hence, one part of the numerical tests we want to discuss is how good the matrices obtained from either compression method approximate the real, unobtainable inverse of the kernel matrix. The second part is dedicated to showcasing the power of the novel symmetric preconditioner introduced in Section 4.2. This is especially done by an application relevant problem in three spatial dimensions.

### 6.1 Setup

Since the theory of localized Lagrange functions was mainly developed for Matérn kernels  $K = \Phi_\nu$ , we will mostly focus on these kernel functions, albeit with varying parameter  $\nu = 0.5, 1.0, 1.5$ . We again refer to Table 1 for explicit formulas, however, for the numerical tests, we choose the length scale parameter  $\delta = 0.1$ , i.e., we consider the radial function  $\Phi_\nu(\cdot/\delta)$ . This could also be considered for the theoretical results presented above, but only leading to different,  $\delta$ -dependent constants.

The set of data sites  $X$  is drawn randomly from a uniform distribution on  $[0, 1]^2$  and we select  $N = 1000, 10\,000, 100\,000$  using the random number generator from the C++ standard library. The fill distance  $h_{X,\Omega}$ , that is important for determining the footprint (12), is then estimated by using a clustering algorithm. Although most of the theoretical results assume quasi-uniform sets of sites, the numerical examples we conducted show that in practice this restriction can be dropped provided that a small regularization term is added. In our experiments, we consider the regularized systems  $\mathbf{M} + \lambda \mathbf{I}$  with  $\lambda = 10^{-6}N$ . Indeed, it is customary to regularize kernel systems since even for a low number of quasi-uniform points the unregularized kernel matrices are notoriously ill conditioned.

The samplet matrix compression is implemented as described in [21]. We compute the samplet compressed matrix using  $q + 1 = 6$  vanishing moments. For the fast assembly of the samplet compressed matrix, we exploit the fast multipole method along as proposed in [21]. The polynomial degree for the degenerate kernel expansion is set to 10 while the cut-off parameter is chosen as  $1/2$  (see [21] for details). After computing the compressed matrix, we apply different sizes of the a-posteriori compression parameter to steer the compression rate of the samplet compressed matrix. Then, we apply a sparse Cholesky decomposition using METIS [28].

All computations have been performed at the Centro Svizzero di Calcolo Scientifico (CSCS) on up to 20 nodes of the Alps cluster with two AMD EPYC 7742 @2.25GHz CPUs and up to 512GB of main memory, resulting in a usage of up to 2560 cores.

## 6.2 Comparing the Compression

We start by providing results on the compression of the inverse matrix. We measure the error in the following way. As explained in Section 4.2, we collect the column vectors  $\beta^{(i)}$  of the matrix  $(\mathbf{A} + \lambda\mathbf{I})^{-1}$  in a global (sparse) matrix  $\mathbf{B}$ . Since this should be a good approximation to the inverse of  $(\mathbf{A} + \lambda\mathbf{I})$ , the error measure

$$\text{error} = \|(\mathbf{A} + \lambda\mathbf{I})\mathbf{B} - \mathbf{I}\|_2,$$

would be best suited to compare the methods. Note that the spectral error is a relative error due to  $\|\mathbf{I}\|_2 = 1$ . To compute the spectral error we use 200 power iterations.

In the theoretical results from Section 4.1, the localization of the Lagrange basis leads to a matrix compression and the resulting error depends on the parameter  $\kappa$  which influences the size of the footprint. However, to compare the numerical results with the samplet compression, we decide to use a different parameter. Since we are mainly interested in how good compressed matrices for the single methods approximate the inverse, we consider the *compression rate*

$$\text{compression rate} = \frac{\text{number of non-zero entries}}{N^2}.$$

This seems to be the right reference value to allow a fair comparison between the methods, since the compression rate directly reflects the memory requirements for the approximate dual basis.

In Fig. 4, we plot the error as a function of the compression rate for the local Lagrange approach. It is interesting to see that the error behaves for every choice of  $\nu$  qualitatively the same and the method seems to converge, achieving good approximation errors even with high compression. The results indicate that the localization of the Lagrange basis yields a simple to implement approach, which gives accuracies dependent just on the compression rate. Indeed, looking at Fig. 4, the error seems to be basically independent of the sample size  $N$  and the smoothness parameter  $\nu$ .

In contrast, as seen in Fig. 5, the compression rate of the samplet method improves as  $N$  increases. The reason for this is that the samplet compression gives a fixed error in basically (i.e., up to a polylogarithmic factor) linear cost, meaning that the compression rate improves as  $N$  increases. This can clearly be observed from Fig. 5. Note that the compression rate specified in this figure is the one of the sparse Cholesky factor since the approximate inverse matrix is symmetric and only half the matrix needs to be stored. When the whole inverse should be stored, the compression rate is twice the given values.

We may conclude from comparing Fig. 4 and Fig. 5 (note that the scaling of the axes is the same) that samplet matrix compression is superior to the local Lagrange basis approach, at least for large data sets. For small data sets, however, the local Lagrange basis approach approximates the inverse matrix quite well and is an attractive alternative since it is much easier to implement than the samplet matrix compression.

## 6.3 Testing the Symmetric Preconditioner

We now turn to testing the new symmetric preconditioner introduced in Section 4.2 using the localized Lagrange basis. We consider the same setup as before but restrict ourselves

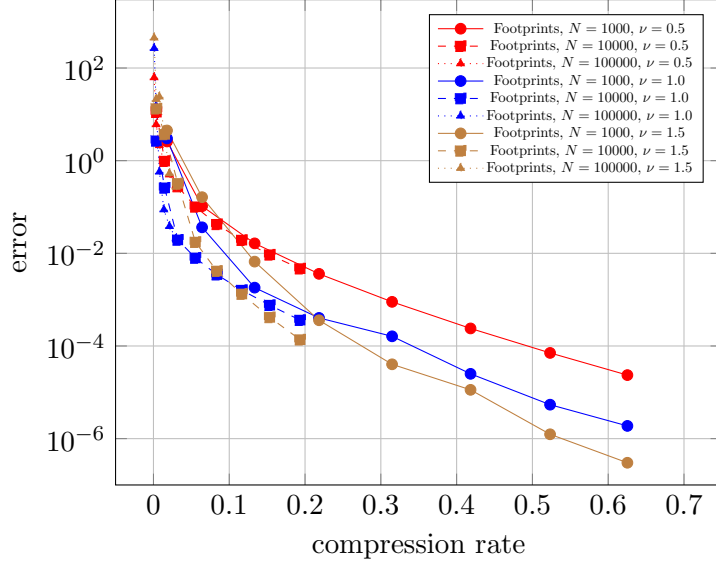


Figure 4: Localized Lagrange approach: Errors as a function of the compression rate in case of varying smoothness parameters  $\nu = 0.5, 1.0, 1.5$  and sample sizes  $N = 10^3, 10^4, 10^5$ .

to a fixed amount of  $N = 100000$  data sites. To assess the quality of the preconditioner, we are interested in comparing the number of (preconditioned) conjugate gradient iterations (see [24] for details) when solving the linear system (2) of equations for the right-hand side given by the vector of all ones versus the footprint parameter  $\kappa$ . To this end, the conjugate gradient method is stopped when the residual is of order  $10^{-9}$ .

$\kappa$	$\#X_j$	Cholesky decomposition			Matrix square root		
		$\nu = 0.5$	$\nu = 1.0$	$\nu = 1.5$	$\nu = 0.5$	$\nu = 1.0$	$\nu = 1.5$
0.5	90	208	339	463	60	63	78
1.0	354	92	136	174	29	28	26
1.5	785	56	77	93	21	18	17
2.0	1374	39	49	58	16	14	13
2.5	2115	30	35	41	14	11	10
3.0	3000	24	28	31	11	10	9

Table 2: Conjugate gradient iterations in case of Cholesky decomposition and the matrix square root versus the footprint size. The matrix square root is more stable since it performs better for the same footprint size, but it requires also more computation time.

We observe from Table 2 that the matrix square root of the footprints provides a better preconditioner compared to their Cholesky decomposition. Indeed, the number of iterations are by about a factor 2-3 smaller for the same footprint size. Nonetheless, the computation of the matrix square root of the footprints is much more expensive compared to their Cholesky decomposition. First, we need only half the memory to store the Cholesky factor compared to the matrix square root. Second, the computation of the matrix square root involves the computation of all eigenvalues and eigenvectors by the QR-method, which is costly. If the problem size does not fit any more into the cache of the computer, we require a factor of about 100 more computation time per footprint for the matrix square root compared to the Cholesky decomposition.

From these experiments, we may thus conclude that the Cholesky decomposition of the footprint matrices provides a good, symmetric preconditioner for large kernel matrices, being superior over the matrix square root approach. We will demonstrate this finding by a further experiment in the next subsection.

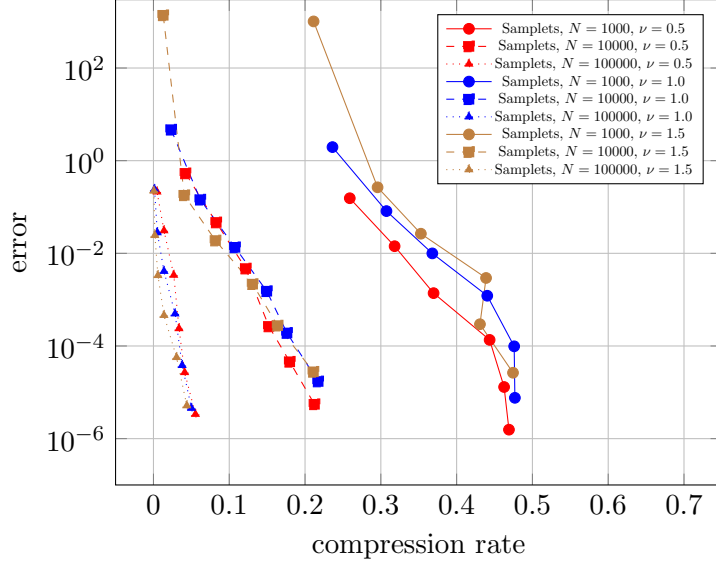


Figure 5: Samplet matrix compression: Errors as a function of the compression rate in case of varying smoothness parameters  $\nu = 0.5, 1.0, 1.5$  and sample sizes  $N = 10^3, 10^4, 10^5$ .

#### 6.4 Signed Distance Function Interpolation

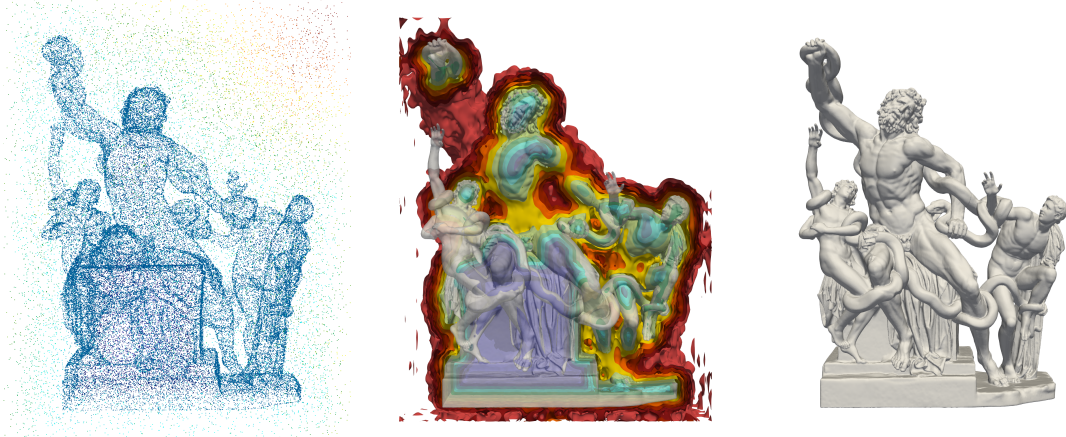


Figure 6: Signed distance function interpolation from a surface mesh of the Laokoon group: Subsample of the signed distance function data (left), levelsets for the values  $\{-5, -4, \dots, 5\}$  (middle) and zero levelset (right).

To demonstrate the capabilities of the developed preconditioner also for real world applications, we consider a signed distance function interpolation problem in three spatial dimensions and the respective surface reconstruction, similarly to [8].

Given a planar triangulation from a 3D scan of the Laokoon group (the scan is provided by the Statens Museum for Kunst), we generate uniform samples of the signed distance by using the about 500 000 vertices the surface mesh and another 250 000 random points within the bounding box of the Laokoon group. This results in  $N = 750\,000$  samples of the signed distance function in total. The left image in Fig. 6 shows a uniform subsample of size 100 000 of the data points. For the interpolation, we consider the exponential kernel  $\Phi_{1/2}$  with lengthscale parameter  $\delta = 0.01$ , where the data sites are rescaled to the hypercube  $(0, 1)^3$ . The kernel matrix is compressed using a hierarchical matrix with adaptive cross approximation, see [3], to compress the far-field of the kernel. The achieved compression

error is  $2.37305 \cdot 10^{-7}$  with a compression rate of 0.009375. The kernel matrix is regularized with a regularization parameter  $\lambda = 10^{-8}N$ .

We use the variant of the preconditioner which is based on the Cholesky decomposition as it has proven to be computationally significantly cheaper than the one which is based on the matrix square root. We set  $\kappa = 0.25$ , which results in a compression rate of 0.000268. The corresponding spectral error is 0.657666 and the conjugate gradient method takes only 12 iterations to achieve a relative residual error of  $5.33355 \cdot 10^{-9}$ .

The interpolated signed distance function is evaluated at a uniform grid with 500 points per axis direction, resulting in 125 000 000 points in total. For the evaluation, we employ the fast multipole method developed in [22] with polynomials of total degree 4 for the degenerate kernel expansion of the kernel in the far-field. The middle image of Fig. 6 shows the levelsets for the values  $\{-5, -4, \dots, 5\}$ , while the zero levelset, corresponding to the reconstructed surface, is found on the right hand side of the figure.

## 7 Conclusion

Motivated by finding dual pairs for finite dimensional subspaces of reproducing kernel Hilbert spaces, we have discussed two methods to approximate the canonical dual pair. On the one hand, we used the exponential decay of the inverse of the Matérn kernel to obtain the local Lagrange functions. The ideas are also applicable to other kernels, those that induce a pseudo-differential operator.

On the other hand, we gave a short overview of the samplet approximation of Lagrange functions, a method that works also for a wider class of kernels, in particular those whose inverse only exhibit algebraic decay.

Both approaches can also be used to compress the (inverse) of the kernel matrix. The matrix resulting from the localized Lagrange functions has already been used for preconditioning of the GMRES method, we, for the first time however, derived a symmetric preconditioner for the kernel matrix of the Matérn kernel. This means that the preconditioner also applies to the conjugate gradient method.

We have presented extensive numerical tests. On the one hand, we have compared the compressive power of the two approaches. Here, we saw that only measuring the compression, the samplet method are clearly superior compared to the local Lagrange basis method. However, the latter method is very easy to implement and is arbitrarily scalable whereas the samplet method needs very sophisticated algorithms to perform. Finally, we have tested the new preconditioning method in an academic example as well as a possible real-live application to demonstrate its feasibility.

**Acknowledgement.** HH and RK were funded in parts by the Swiss National Science Foundation through the grant “Adaptive Boundary Element Methods Using Anisotropic Wavelets” (200021\_192041). MM was funded in parts by the SNSF starting grant “Multiresolution methods for unstructured data” (TMSGI2\_211684).

## References

- [1] D. Alm, H. Harbrecht, and U. Krämer. The  $\mathcal{H}^2$ -wavelet method. *Journal of Computational and Applied Mathematics*, 267:131–159, 2014.
- [2] N. Angleitner, M. Faustmann, and J.M. Melenk.  $\mathcal{H}$ -inverses for rbf interpolation. *Advances in Computational Mathematics*, 49:85, 2023.
- [3] M. Bebendorf and S. Rjasanow. Adaptive low-rank approximation of collocation matrices. *Computing*, 70(1):1–24, 2003.
- [4] G. Beylkin. Wavelets, multiresolution analysis and fast numerical algorithms. In G. Erlebacher, M.Y. Hussaini, and L.M. Jameson, editors, *Wavelets Theory and Applications*, pages 182–262, Oxford, 1996. Oxford University Press.
- [5] G. Beylkin, R. Coifman, and V. Rokhlin. Fast wavelet transforms and numerical algorithms I. *Communications on Pure and Applied Mathematics*, 44(2):141–183, 1991.

- [6] L. Boutet de Monvel and P. Krée. Pseudo-differential operators and Gevrey classes. *Université de Grenoble. Annales de l'Institut Fourier*, 17(fasc. 1):295–323, 1967.
- [7] Martin Buhmann and Janin Jäger. *Quasi-Interpolation*. Cambridge Monographs on Applied and Computational Mathematics. Cambridge University Press, 2022.
- [8] J. C. Carr, R. K. Beatson, J. B. Cherrie, T. J. Mitchell, W. R. Fright, B. C. McCallum, and T. R. Evans. Reconstruction and representation of 3D objects with radial basis functions. In *Proceedings of the 28th annual conference on Computer graphics and interactive techniques*, SIGGRAPH '01, pages 67–76, New York, 2001. Association for Computing Machinery.
- [9] W. Dahmen, H. Harbrecht, and R. Schneider. Compression techniques for boundary integral equations. asymptotically optimal complexity estimates. *SIAM Journal on Numerical Analysis*, 43(6):2251–2271, 2006.
- [10] Stefano De Marchi and Holger Wendland. On the convergence of the rescaled localized radial basis function method. *Applied Mathematics Letters*, 99:105996, 2020.
- [11] G.E. Fasshauer. *Meshfree Approximation Methods with MATLAB*. World Scientific, River Edge, 2007.
- [12] E. Fuselier, T. Hangelbroek, F.J. Narcowich, J.D. Ward, and G.B. Wright. Localized bases for kernel spaces on the unit sphere. *SIAM Journal on Numerical Analysis*, 51(5):2538–2562, 2013.
- [13] A. George. Nested dissection of a regular finite element mesh. *SIAM Journal on Numerical Analysis*, 10(2):345–363, 1973.
- [14] W. Hackbusch. A sparse matrix arithmetic based on  $\mathcal{H}$ -matrices. Part I: Introduction to  $\mathcal{H}$ -matrices. *Computing*, 62(2):89–108, 1999.
- [15] W. Hackbusch. *Hierarchical Matrices: Algorithms and Analysis*. Springer, Berlin-Heidelberg, 2015.
- [16] W. Hackbusch and B.N. Khoromskij. A sparse matrix arithmetic based on  $\mathcal{H}$ -matrices. Part I: Application to multi-dimensional problems. *Computing*, 64(1):27–47, 2000.
- [17] N. Hale, N.J. Higham, and L.N. Trefethen. Computing  $\mathbf{a}^\alpha$ ,  $\log(\mathbf{a})$ , and related matrix functions by contour integrals. *SIAM Journal on Numerical Analysis*, 5(46):2505–2523, 2008.
- [18] T. Hangelbroek, F.J. Narcowich, C. Rieger, and J.D. Ward. An inverse theorem on bounded domains for meshless methods using localized bases. *ArXiv e-prints*, 2014.
- [19] T. Hangelbroek, F.J. Narcowich, X. Sun, and J.D. Ward. Kernel approximation on manifolds ii: The  $l_\infty$  norm of the  $l_2$  projector. *SIAM Journal on Mathematical Analysis*, 43(2):662–684, 2011.
- [20] Thomas Hangelbroek, Francis Narcowich, Christian Rieger, and Joseph Ward. An inverse theorem for compact lipschitz regions in  $\mathbb{R}^d$  using localized kernel bases. *Mathematics of Computation*, 87(312):1949–1989, 2018.
- [21] H. Harbrecht and M. Multerer. Samplers: Construction and scattered data compression. *Journal of Computational Physics*, 471:111616, 2022.
- [22] H. Harbrecht, M. Multerer, and J. Quizi. The dimension weighted fast multipole method for scattered data approximation. *arXiv:2402.09531*, 2024.
- [23] Helmut Harbrecht, Multerer Multerer, Olaf Schenk, and Christoph Schwab. Multiresolution kernel matrix algebra. *Numerische Mathematik*, 3(156):1085–1114, 2024.
- [24] Magnus R. Hestenes and Eduard Stiefel. Methods of conjugate gradients for solving linear systems. *Journal of Research of the National Institute of Standards*, 49:409–436, 1952.
- [25] L. Hörmander. *The analysis of linear partial differential operators. III*. Classics in Mathematics. Springer, Berlin, 2007. Pseudo-differential operators, Reprint of the 1994 edition.
- [26] Lars Hörmander. *The analysis of linear partial differential operators. I*. Classics in Mathematics. Springer, Berlin, 2003. Distribution theory and Fourier analysis, Reprint of the second (1990) edition.

- [27] A.S. Householder. *The Theory of Matrices in Numerical Analysis*. Blaisdell, New York, 1964.
- [28] G. Karypis and V. Kumar. Metis: A software package for partitioning unstructured graphs, partitioning meshes, and computing fill-reducing orderings of sparse matrices. Technical Report 97-061, Department of Computer Science, University of Minnesota, 1997.
- [29] Paul Krée. Les noyaux des opérateurs pseudo-différentiels classiques (OPDC). *Université de Grenoble. Annales de l'Institut Fourier*, 19(fasc. 1):179–194 x, 1969.
- [30] G. Leobacher and F. Pillichshammer. *Introduction to Quasi-Monte Carlo Integration and Applications*. Springer International Publishing, Cham, 2010.
- [31] L. Lin, C. Yang, J. C. Meza, J. Lu, L. Ying, and W. E. Selin—*an algorithm for selected inversion of a sparse symmetric matrix*. *ACM Transactions on Mathematical Software*, 37(4):40, 2011.
- [32] R.J. Lipton, D.J. Rose, and R.E. Tarjan. Generalized nested dissection. *SIAM Journal on Numerical Analysis*, 16(2):346–358, 1979.
- [33] S.G. Mallat. A theory for multiresolution signal decomposition: The wavelet representation. *IEEE Transactions on Pattern Analysis and Machine Intelligence*, 2(7), 1989.
- [34] Bertil Matérn. *Spatial variation*, volume 36 of *Lecture Notes in Statistics*. Springer, Berlin, second edition, 1986.
- [35] Stefan Müller and Robert Schaback. A newton basis for kernel spaces. *Journal of Approximation Theory*, 161(2):645–655, 2009.
- [36] Maryam Pazouki and Robert Schaback. Bases for kernel-based spaces. *Journal of Computational and Applied Mathematics*, (236):575–588, 2011.
- [37] Luigi Rodino. *Linear partial differential operators in Gevrey spaces*. World Scientific Publishing Co., Inc., River Edge, NJ, 1993.
- [38] H. Rue and L. Held. *Gaussian Markov Random Fields: Theory and Applications*, volume 104 of *Monographs on Statistics and Applied Probability*. Chapman & Hall / CRC press, London, 2005.
- [39] Youcef Saad and Martin H. Schultz. GMRES: A Generalized Minimal Residual Algorithm for solving nonsymmetric linear systems. *SIAM Journal on Scientific and Statistical Computing*, 7:856–869, 1986.
- [40] R. Schneider and T. Weber. Wavelets for density matrix computation in electronic structure calculation. *Applied Numerical Mathematics*, 56(10-11):1383–1396, 2006.
- [41] G. Schulz. Iterative Berechnung der reziproken Matrix. *ZAMM – Journal of Applied Mathematics and Mechanics*, pages 57–59, 1933.
- [42] R.T. Seeley. Topics in pseudo-differential operators. In *Pseudo-Differential Operators (C.I.M.E., Stresa, 1968)*, page 167–305. Edizioni Cremonese, Rome, 1969.
- [43] Ingo Steinwart and Andreas Christmann. *Support Vector Mashines*. Information Science and Statistics. Springer, New York, 2008.
- [44] J. Tausch and J. White. Multiscale bases for the sparse representation of boundary integral operators on complex geometry. *SIAM Journal on Scientific Computing*, 24(5):1610–1629, 2003.
- [45] M.E. Taylor. *Pseudodifferential operators*, volume 34 of *Princeton Mathematical Series*. Princeton University Press, Princeton, NJ, 1981.
- [46] Holger Wendland. *Scattered Data Approximation*. Cambridge Monographs on Applied and Computational Mathematics. Cambridge University Press, Cambridge, 2004.